Measurement of the two-time intensity-correlation function of arbitrary states

Katarina Stensson[*] and Gunnar Björk

Department of Applied Physics, Royal Institute of Technology (KTH) AlbaNova University Center, SE - 106 91 Stockholm, Sweden

For light-intensity-correlation measurements, different methods are used in the high-photon-number or high-intensity regime and in the single- and two-photon regime. Hence, there is an unfortunate measurement "gap" primarily for multiphoton, quantum states. These states, for example, multiphoton Fock states, will be increasingly important in the realization of quantum technologies and in exploring the boundaries between quantum and classical optics. We show that a naïve approach based on attenuation, state splitting, and two-detector correlation can give the correct two-time intensity correlation for any state. We analyze how added losses decrease the measurement systematic error. The price to be paid is that the losses increase the measurement statistical error or, alternatively, increase the acquisition time for a given tolerable level of statistical error. We have experimentally demonstrated the feasibility of the method for a coherent state and a quasithermal state. The method is easy to implement in any laboratory and will simplify characterization of medium and highly excited nonclassical states as they become experimentally available.

I. INTRODUCTION

Photon-correlation measurements were pioneered in the 1950s by Hanbury Brown and Twiss, and described quantum mechanically by Glauber a few years later [1,2]. Glauber did not only explain the Hanbury-Brown–Twiss (HBT) effect, but pointed out that the fourth-order (in field amplitude, however, often referred to as second order, then referring to intensity) autocorrelation function offers the possibility of observing the uniquely quantum mechanical effect of antibunching. This effect was first demonstrated experimentally in 1977, and has since then been used to prove the "quantumness" of many single- and two-photon sources [3–9]. In addition to Glauber's theory, semiclassical descriptions of the detection process contributed to understanding the photon-correlation effects, and to relate the correlation functions to quantities scientists could actually measure in the laboratory [10,11]. For classical light, the fourth-order correlation function $g^{(4)}(\tau)$, defined in Eq. (2) below, has a direct relation to the measurement of four fields (or two intensities). For nonclassical light the relation is more complicated because of the different possible ordering of the correlation functions, and noncommutability of the associated quantum operators. Normal ordering results in the correlation function containing the term $\langle \hat{n}^2 \rangle$, suggesting measurement of the operator $\hat{n}^2$ with eigenvalues $1, 4, 9, 16, \ldots$, which is not straightforward.

The standard way of measuring $g^{(4)}(\tau)$ for weak light is by splitting the light beam and detecting coincidences between the two paths, either through a start-stop type measurement or using a coincidence module. Some of the first experiments to verify Glauber's theory for coherent and Gaussian light used a time-to-amplitude converter (TAC) [12]. The TAC method, however, like other start-stop type measurements, gives the probability of detecting one photon and then *the next photon*

after a time interval τ, rather than the probability of detecting *a photon* after a time interval τ. The former falls off exponentially outside the time interval where $\langle \hat{n} \rangle \ll 1$, while the latter has a more direct relation with the fourth-order correlation function [13,14]. Coincidence measurements correspond more closely to the latter, but are limited by the time resolution of the coincidence modules. Consequently, these methods require that the measured light contains no more than one photon, either within the time-resolved coincidence window or within the time interval τ under investigation. This has limited the application of the fourth-order correlation function to mainly single-photon states and other weakly excited light. At the other end, the intensity-correlation function for classical, highly excited light ($\langle n \rangle \gtrsim 10$) can be measured directly with cameras [15] or pin-diodes [16], or by two-photon absorption in semiconductors [17]. However, for "mesoscopic" states lying in between these two extremes, suitable methods for correlation measurements are lacking.

It is of increasing importance to find strategies to characterize quantum mechanical states containing more than two photons, as such states are interesting for numerous quantum technology applications [18–20] and for exploring the boundaries between quantum and classical physics [21–23]. Since efficient number resolving detectors are not readily available (see, for example, [24,25]), the most common method used today to measure high-n number states or their superpositions is n-fold coincidence measurement [26–30]. This method ensures that n photons are present, but not the presence of an n-photon number state. Other measurement techniques include those of higher order correlation functions by time or spatial multiplexing [31,32], also combined with homodyne detection [33]. The setups required for the above-mentioned measurements increase in complexity with the size of the number state measured.

It is also interesting to note that it used to be common practice to specify under which conditions the results of

————
[*]stenss@kth.se

fourth-order correlation measurement were accurate (see, for example, [7,13]). This practice has been dropped by many experimentalists, and it seems in some cases that the nondirect relation between what is measured in the laboratory and the theoretical $g^{(4)}(\tau)$ is either lost or ignored. As efficiencies of detectors and experimental setups improve, it becomes important to keep in mind that the result of HBT type measurements resembles less and less the theoretical $g^{(4)}(\tau)$.

In this paper we investigate the effect of loss on the fourth-order correlation function of arbitrary states, when measured in a Hanbury-Brown–Twiss type setup. It is well known that $g^{(4)}(\tau)$ is robust under loss. Still, we find it surprising that the fourth-order quantum correlations not only completely survive the loss, so that the loss-affected state "remembers" the properties of the initial state, but that introducing loss even provides access to information formerly hard to attain about a whole set of states. Although excess attenuation has formerly been used to extend the dynamic range of measurements [34,35], the finding that the systematic error in $g^{(4)}$ measurements can be reduced with attenuation has not to our knowledge been exploited to address the difficulties in measuring the fourth-order correlation function of medium and highly excited states.

We show the somewhat counterintuitive result that the precision in $g^{(4)}$ measurements can increase when loss is introduced in the setup. This is true for any state, and for measurements using ideal (photon number resolving) detectors as well as ordinary "click" detectors. However, the cost of decreasing the systematic error in $g^{(4)}(\tau)$ is an increase in the statistical error. We introduce the measured normalized coincidences $\gamma^{(4)}(\tau)$ as a function of the total quantum efficiency of the setup, and show that $\gamma^{(4)}(0) \to g^{(4)}(0)$ as the quantum efficiency approaches zero. The theoretical results are analyzed for various states and experimentally supported by measurements of the correlation function of coherent states and quasithermal states. This finding leads us to propose excess attenuation as a method to improve the accuracy in $g^{(4)}$ measurement and expand its use to a larger set of states.

II. FOURTH-ORDER CORRELATION FUNCTION

For a state $\hat{\rho}$, the normally ordered, two-time, fourth-order autocorrelation function is defined as [14]

$$G^{(4)}(t,\tau) = \mathrm{Tr}[\hat{\rho}\hat{a}^{\dagger}(t)\hat{a}^{\dagger}(t+\tau)\hat{a}(t+\tau)\hat{a}(t)], \quad (1)$$

or in normalized form

$$g^{(4)}(t,\tau) = \frac{\mathrm{Tr}[\hat{\rho}\hat{a}^{\dagger}(t)\hat{a}^{\dagger}(t+\tau)\hat{a}(t+\tau)\hat{a}(t)]}{\mathrm{Tr}[\hat{\rho}\hat{a}^{\dagger}(t)\hat{a}(t)]\mathrm{Tr}[\hat{\rho}\hat{a}^{\dagger}(t+\tau)\hat{a}(t+\tau)]}, \quad (2)$$

where $\hat{a}$ ($\hat{a}^{\dagger}$) is the annihilation (creation) operator. (Quite often this coherence function is referred to as a second-order correlation function because classically it represents the correlation between two intensities.) For a stationary ensemble of states, there is no time dependence in the above equation, so $g^{(4)}(t,\tau) = g^{(4)}(\tau)$ at all times. It is well known that for a single-mode number state $|n\rangle$ this function equals $1 - 1/n$ at $\tau = 0$. For a coherent state the function equals unity at all times, and for a single-mode thermal state the function equals 2 when $\tau = 0$. For sufficiently long times (much longer than
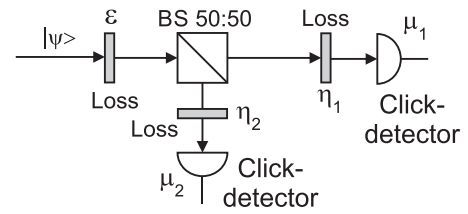

FIG. 1. Proposed measurement setup to measure the fourth-order correlation function of the state $|\psi\rangle$. BS denotes the beam splitter.

the coherence time of the state) the normalized, fourth-order correlation function tends to unity for any state.

III. SETUP

The setup, a standard HBT interferometer with attenuation introduced, is outlined in Fig. 1. The state to be measured is first attenuated so that a fraction $1 - \epsilon^2$ is absorbed and ϵ^2 is transmitted. The attenuated state then impinges on a 50:50 beam splitter that divides the state into two equal halves. Each half subsequently passes a linear absorber (e.g., a neutral density filter) which transmits a fraction η_i^2 where $i = 1,2$ and absorbs the rest. The pre-beam-splitter attenuation is intentional (but also includes any unintentional loss, e.g., due to poor coupling between the generated and measured mode). The post-beam-splitter loss models unintentional losses when coupling the beam-splitter output to the respective detectors. The transmitted photons are measured by two photodetectors of the click-detector type. That is, the detectors will only distinguish between no photons and one or more photons. Moreover, we shall assume that they do not even do this task perfectly.

The click detector is modeled through its single-photon quantum efficiency μ^2. If two photons impinge on the detector, three things can happen: no, one, or two photons may be "lost" or "unseen" by the detector. The probability for the three cases are μ^4, $2\mu^2(1 - \mu^2)$, and $(1 - \mu^2)^2$. It is only when both photons are lost that the detector does not fire. Generalizing to n photons, the probability $P(n)$ to get the detector to fire is

$$P(n) = \sum_{m=1}^{n} \frac{n!}{(n-m)!m!}(1 - \mu^2)^{(n-m)}\mu^{2m} = 1 - (1 - \mu^2)^n. \quad (3)$$

This probability will be used in the following.

IV. ARBITRARY STATE INPUT

Now we want to see if we can replicate the normalized, fourth-order correlation function in Eq. (2) with the proposed setup and two-click detectors. Consider a normalized, pure state. The purity restriction will soon be seen to be irrelevant for what follows. All pure states can be expanded in the number state basis as

$$|\psi\rangle = \sum_{n=0}^{\infty} c_n|n\rangle, \quad (4)$$

where c_n are complex probability amplitudes. According to the definition the normally ordered, fourth-order, normalized

correlation function at zero time difference for such a state is

$$g^{(4)}(\tau = 0) = \frac{\sum_{n=2}^{\infty} |c_n|^2 n(n-1)}{\left(\sum_{n=1}^{\infty} |c_n|^2 n\right)^2}. \qquad (5)$$

We introduce the normalized coincidences $\gamma^{(4)}$ and write the expression for the measurement outcome for our proposed measurement of $g^{(4)}(\tau = 0)$ as

$$\gamma^{(4)}(\tau = 0) = \frac{P(\text{Coinc.})}{P(\text{Click}_1)P(\text{Click}_2)}, \qquad (6)$$

where $P(\text{Coinc.})$ is the probability to record a coincidence detection, and $P(\text{Click}_j)$ the probability to get a click in detector j. For the pure state in Eq. (4) the above function can be expressed as

$$\gamma^{(4)}(\tau = 0) = \frac{\sum_{n=2}^{\infty} |c_n|^2 P(\text{Coinc.}|n)}{\left[\sum_{n=1}^{\infty} |c_n|^2 P(\text{Click}_1|n)\right]\left[\sum_{n=1}^{\infty} |c_n|^2 P(\text{Click}_2|n)\right]}. \qquad (7)$$

Let us look at the n-photon term. If the input state is the number state $|n\rangle$, then after the first attenuator, modeling any linear transmission or coupling loss, the probability of getting k photons through is

$$P(k|n) = \frac{n!}{(n-k)!k!}(1-\epsilon^2)^{(n-k)}\epsilon^{2k}, \qquad (8)$$

where $0 \leqslant k \leqslant n$. After the 50:50 beam splitter (BS) the probability of getting $k-m$ photons in one output, and m photons in the other output, given that k photons entered the BS is

$$P(k-m,m|k) = \frac{k!}{2^k(k-m)!m!}, \qquad (9)$$

where $0 \leqslant m \leqslant k$. Moving on to the next step, we now have a state $|k-m,m\rangle$ incident on the two absorbers in Fig. 1. The probability that l photons are transmitted through the absorber in the first path and q photons are transmitted in the second path is

$$P(l,q|k-m,m) = \frac{\left(1-\eta_1^2\right)^{(k-m-l)}\eta_1^{2l}\left(1-\eta_2^2\right)^{(m-q)}\eta_2^{2q}(k-m)!m!}{(k-m-l)!l!(m-q)!q!}, \qquad (10)$$

where $0 < l < k-m$ and $0 \leqslant q \leqslant m$. If a state with l photons is incident on a click detector that has the single-photon quantum efficiency μ_j^2, then the probability of not getting a click will be $(1-\mu_j^2)^l$, according to Eq. (3). Summing over all possibilities of getting l and q photons given that $m-k$ and m photons were impinging on attenuators η_1 and η_2, we get the probability for no click as

$$P(\text{No click}|k-m,k) = \sum_{l=0}^{k-m}\sum_{q=0}^{m} P(l,q|k-m,m)\left(1-\mu_1^2\right)^l\left(1-\mu_2^2\right)^q = \left(1-\eta_1^2\mu_1^2\right)^{k-m}\left(1-\eta_2^2\mu_2^2\right)^m. \qquad (11)$$

We can now figure the probability of getting a coincidence click given that k photons are incident on the 50:50 beam splitter by summing over all possibilities that $k-m$ photons take output 1 and m photons exit output 2 as

$$P(\text{Coinc.}|k) = \sum_{m=0}^{k} P(k-m,m|k)\left(1-\left[1-\eta_1^2\mu_1^2\right]^{k-m}\right)\left(1-\left[1-\eta_2^2\mu_2^2\right]^m\right)$$

$$= 1 - \left(1-\frac{\eta_1^2\mu_1^2}{2}\right)^k - \left(1-\frac{\eta_2^2\mu_2^2}{2}\right)^k + \left(1-\frac{\eta_1^2\mu_1^2}{2}-\frac{\eta_2^2\mu_2^2}{2}\right)^k. \qquad (12)$$

Finally, by summing over all possibilities to get k photons through the attenuator preceding the beam splitter we get

$$P(\text{Coinc.}|n) = \sum_{k=0}^{n} P(k|n)P(\text{Coinc.}|k) = 1 - \left(1-\frac{\epsilon^2\eta_1^2\mu_1^2}{2}\right)^n - \left(1-\frac{\epsilon^2\eta_2^2\mu_2^2}{2}\right)^n + \left(1-\frac{\epsilon^2}{2}\left[\eta_1^2\mu_1^2+\eta_2^2\mu_2^2\right]\right)^n. \qquad (13)$$

Note that this expression vanishes for $n = 0,1$. (If $\epsilon^2 = \eta_1^2 = \eta_2^2 = \mu_1^2 = \mu_2^2 = 1$, then the last term on the right-hand side reads 0^n, which strictly speaking is mathematically undefined for $n = 0$. However, in this context the expression must be interpreted or defined as unity for $n = 0$). When the input state $|n\rangle$ is propagated through the whole setup in Fig. 1 it gives rise to the following six-mode state, with the photons

in the first and second mode from the left modeling the (now ideal) detector, and the rest of the photons divided between the five loss modes: $|l,q,k,m,o,n-(l+q+k+m+o)\rangle$, where l,q,k,m,o are all non-negative integers and $l+q+k+m+o \leqslant n$. These two conditions ensure that all possible final states are distinguishable, so that they do not interfere with each other. Hence, the final result will be the same whether

the state is mixed or pure, provided that the probabilities $|c_n|^2$ correspond to the diagonal elements ρ_{nn} in a mixed state, if the latter is expressed in the number basis. We can therefore make the computation assuming a pure state input, knowing that the result will be valid also for any mixed state after making the substitution $|c_n|^2 \to \rho_{nn}$. To estimate the normalized, fourth-order correlation function we should also compute the probability of obtaining a click at either detector, irrespective of whether the other detector clicks or not. These probabilities can be obtained in the same manner as the coincidence probability was obtained. They are

$$P(\text{Click}_j|n) = 1 - \left(1 - \frac{\epsilon^2 \eta_j^2 \mu_j^2}{2}\right)^n, \qquad (14)$$

where $j = 1,2$ denotes the particular detector clicking. The click probabilities in Eqs. (13) and (14) complete the expression in Eq. (7). If we assume that the detectors have the same effective quantum efficiencies, $\eta_1^2 \mu_1^2 = \eta_2^2 \mu_2^2 = \eta^2$, the expression can be simplified to

$$\gamma^{(4)}(0) = \frac{\sum_{n=2}^{\infty} |c_n|^2 (1 - 2[1 - \epsilon^2 \eta^2/2]^n + [1 - \epsilon^2 \eta^2]^n)}{\left(\sum_{n=1}^{\infty} |c_n|^2 [1 - \{1 - \epsilon^2 \eta^2/2\}^n]\right)^2}. \qquad (15)$$

Equations (7) and (15) will asymptotically approach the right-hand side of Eq. (5) for most states when the conditions $\epsilon^2 \eta_j^2 \mu_j^2 \ll 1/\langle \hat{n} \rangle$, $j = 1,2$, where $\langle \hat{n} \rangle$ is the average photon number of the state. In other words, adding additional attenuation leads to a higher resemblance between the measured $\gamma^{(4)}(\tau)$ and the fourth-order correlation function for that state. According to the above calculation, this is true for any state, and the fourth-order coherence properties of quantum states (as well as classical) are preserved, or even revealed, when exposed to extensive loss. However, for some "exotic" states, e.g., the state

$$|\psi\rangle_p = \sqrt{1 - |c_N|^2}|0\rangle + c_N|N\rangle, \qquad (16)$$

for which $\langle \hat{n} \rangle = |c_N|^2 N$, one needs to fulfill the more stringent condition $\eta_j^2 \ll 1/N$, $j = 1,2$ before the measurement result at $\tau = 0$ converges to the correct value. However, experimentally one only needs to increase the loss $1 - \epsilon^2$ until the measurement result converges toward a fixed number to reach the correct correlation-function value. Hence, there is no need to have *a priori* knowledge of the measured state. Thus, we have shown that our proposed experimental method will work for any arbitrary state. In the coming sections we will look more closely at Eq. (15) for some specific classes of states.

V. NUMBER STATE INPUT

Using the intermediate results in Sec. IV and letting ϵ^2 approach zero we get the lowest order term of the coincidence and click probabilities for a number state:

$$\lim_{\epsilon^2 \to 0} P(\text{Coinc.}|n) = \frac{\epsilon^4 \eta_1^2 \eta_2^2 \mu_1^2 \mu_2^2}{4}(n^2 - n), \qquad (17)$$

$$\lim_{\epsilon^2 \to 0} P(\text{Click}_j|n) = \frac{\epsilon^2 \eta_j^2 \mu_j^2 n}{2}. \qquad (18)$$
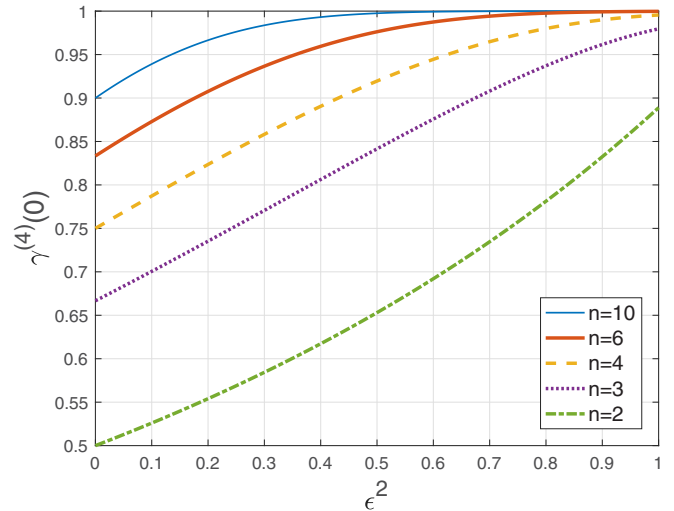

FIG. 2. Number states: calculated normalized coincidences $\gamma_n^{(4)}(0)$ for different n, as a function of attenuation [Eq. (20)]. Here we assume $\eta_1^2 \mu_1^2 = \eta_2^2 \mu_2^2$ and that they are included in ϵ^2 for simplicity.

Thus, if one now adjusts the attenuation ϵ^2 so that $\epsilon^2 \eta_j^2 \mu_j^2 n$ is much smaller than unity for both detectors, then the ratio between the coincidence probability and the product of the individual detectors' respective click probabilities approaches

$$\gamma_n^{(4)}(0) = \frac{P(\text{Coinc.}|n)}{P(\text{Click}_1|n)P(\text{Click}_2|n)} \to 1 - \frac{1}{n}. \qquad (19)$$

This is the expected result when measuring $g^{(4)}(\tau = 0)$ for a number state.

At the opposite end, when $\tau \to \infty$, we instead have $\gamma^{(4)}(\tau \to \infty) = 1$ for any state, because the correlation at sufficiently long time is lost and the numerator therefore factors and becomes identical to the denominator of $g^{(4)}(\tau)$.

For a specific number state $|n\rangle$ as input and assuming equal detector efficiencies and losses in the two paths, Eq. (15) simplifies to

$$\gamma_n^{(4)}(0) = \frac{1 - 2(1 - \epsilon^2 \eta^2/2)^n + (1 - \epsilon^2 \eta^2)^n}{(1 - [1 - \epsilon^2 \eta^2]^n)^2}. \qquad (20)$$

Equation (20) is plotted for number states of different n in Fig. 2. It shows a strong dependence on the quantum efficiency of the setup, and allows an estimation of the efficiency required for certain precision in $g^{(4)}$ measurements. The nonzero dead times of the detectors, as well as the resolution of the coincidence circuit, are other factors that motivate a low quantum efficiency, but these are separate from the effect in the result obtained here. We can also show (although the full derivation is omitted here) that photon number resolving detectors do not improve the situation. Rather, using ordinary Avalanche photo-diodes (APDs) or other nonideal detectors leads to a more rapid convergence between $\gamma^{(4)}$ and $g^{(4)}$ then if ideal, photon number resolving detectors are used, as can be seen for two-photon number states in Fig. 3.

VI. COHERENT STATE INPUT

The coherent state and its photon count statistics are the result of a memoryless system. Hence, if a coherent state is
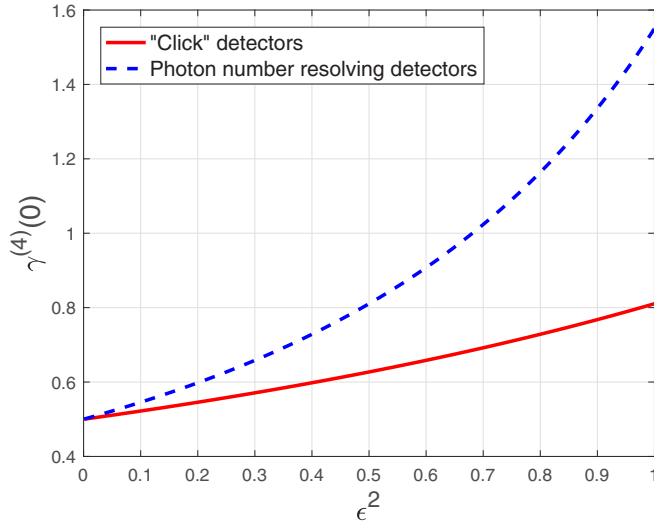
FIG. 3. Number states: calculated normalized coincidences $\gamma_n^{(4)}(0)$ when using ordinary "click" detectors (red) and photon number resolving detectors (blue).

split in two, the output state is in a separable state of two coherent states. Likewise, if a coherent state is subject to linear loss, the transmitted state is a coherent state with reduced field amplitude. Thus, even at $\tau = 0$, in this case there is no correlation between the photons falling onto the two detectors, so that we get $P(\text{Coinc.}) = P(\text{Click}_1)P(\text{Click}_2)$. This means that the ratio

$$\gamma_{\text{coh}}^{(4)}(\tau = 0) = \frac{P(\text{Coinc.})}{P(\text{Click}_1)P(\text{Click}_2)} = 1, \qquad (21)$$

which is agreement with $g^{(4)}(\tau = 0)$ for coherent states.

A. Measuring the fourth-order correlation function for a coherent state

The correlation function was measured for a coherent state by coupling a 632-nm HeNe laser into a single-mode fiber, connected to a fiber beam splitter with splitting ratio close to 50:50 at 632 nm. The two outputs were detected by two APDs. Attenuation in the form of neutral density filters (with transmission in the range $\epsilon^2 = 0.16$–1) were inserted before the laser was coupled into the fiber. The normalized coincidences $\gamma^{(4)}(\tau)$ were measured for different attenuation strengths as a function of the time delay τ between the arrival times at the two detectors, shown in Fig. 4.

The result shows no correlation in time, or as a function of attenuation, as expected. Error bars represent statistical errors. The x axis in Fig. 4 is scaled to include losses in the fiber and at the detector, as well as the variable part of ϵ^2. Since $\langle \hat{n} \rangle$ and the quantum efficiency occur together in the formulas (a loss in one is a gain in the other) only an approximate value of the total quantum efficiency can be found by estimating the total loss in the setup.

VII. THERMAL STATE INPUT

To compute the probabilities $P(\text{Coinc.})$ and $P(\text{Click}_i)$ for a thermal input state we use the fact that the thermal state,
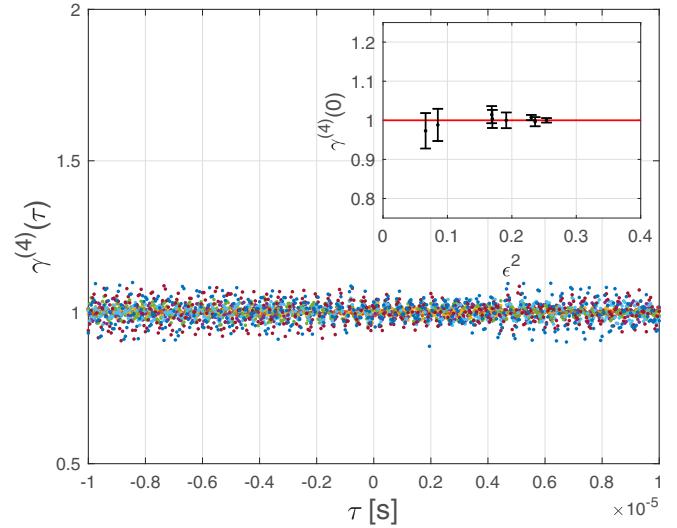

FIG. 4. Coherent state: Measured normalized coincidences $\gamma^{(4)}(\tau)$, for several attenuations ϵ^2 (different colored dots, $T = 0.16$–1), as a function of delay time show no correlations. The inset shows measured $\gamma^{(4)}(\tau = 0)$ for different attenuations ϵ^2. The red line is the theoretically expected value. Bars represent the statistical error.

expressed in the number state basis, is simply an exponential statistical distribution of number states. Hence, if the thermal-state mean photon number is denoted $\langle \hat{n} \rangle$, then

$$P(\text{Coinc.}) = \frac{1}{1 + \langle \hat{n} \rangle} \sum_{n=0}^{\infty} \left(\frac{\langle \hat{n} \rangle}{1 + \langle \hat{n} \rangle} \right)^n P(\text{Coinc.}|n)$$

$$= 1 - \frac{1}{1 + \langle \hat{n} \rangle \epsilon^2 \eta_1^2 \mu_1^2 / 2} - \frac{1}{1 + \langle \hat{n} \rangle \epsilon^2 \eta_2^2 \mu_2^2 / 2}$$

$$+ \frac{1}{1 + \langle \hat{n} \rangle \epsilon^2 \left(\eta_1^2 \mu_1^2 + \eta_2^2 \mu_2^2 \right) / 2}, \qquad (22)$$

and

$$P(\text{Click}_j) = \frac{1}{1 + \langle \hat{n} \rangle} \sum_{n=0}^{\infty} \left(\frac{\langle \hat{n} \rangle}{1 + \langle \hat{n} \rangle} \right)^n P(\text{Click}_j|n)$$

$$= 1 - \frac{1}{1 + \langle \hat{n} \rangle \epsilon^2 \eta_j^2 \mu_j^2 / 2}. \qquad (23)$$

The lowest order expansion terms of these two functions as $\epsilon^2 \to 0$ are

$$P(\text{Coinc.}) \to \langle \hat{n} \rangle^2 \epsilon^4 \eta_1^2 \eta_2^2 \mu_1^2 \mu_2^2 / 2 \qquad (24)$$

and

$$P(\text{Click}_j) \to \langle \hat{n} \rangle \epsilon^2 \eta_j^2 \mu_j^2 / 2. \qquad (25)$$

Hence, when $\epsilon^2 \to 0$, the estimated normalized, fourth-order correlation function at $\tau = 0$ for a thermal state approaches

$$\gamma_{\text{th}}^{(4)}(\tau = 0) = \frac{P(\text{Coinc.})}{P(\text{Click}_1)P(\text{Click}_2)} \to 2, \qquad (26)$$

which also is the expected value for a thermal state. We have plotted $\gamma_{th}^{(4)}(0) = P(\text{Coinc.})/P(\text{Click}_1)P(\text{Click}_2)$ in Fig. 6 for different average photon numbers, calculated from the expressions in Eqs. (22) and (23).
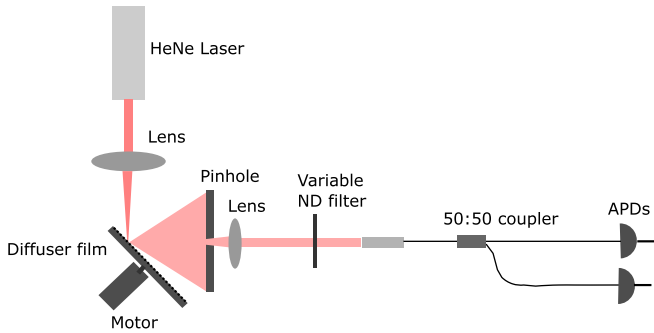
FIG. 5. Setup to generate and detect $\gamma^{(4)}(\tau)$ for a quasithermal state. $v_{\text{rot}} = 105$ rad/s, the average diffuser film grain size is 5 μm.

A. Measuring the fourth-order correlation function for a quasithermal state

A setup as in Fig. 5 was constructed to measure the fourth-order correlation function of a quasithermal state. The state was generated by focusing a HeNe laser with $\lambda = 632$ nm (the same laser generating the coherent state above) onto a diffuser film with average grain size $d = 5$ μm, rotating at around 105 rad/s. Part of the light generated was collected in a fiber, and split in two paths by a fiber beam splitter with splitting ratio close to 50:50, before being detected by two APDs. The same delay generator and coincidence module as before was used to vary the delay time τ and detect coincidences. The attenuation ϵ^2 was introduced as neutral density filters with varying transmittance, before the light was coupled into the fiber.

The result $\gamma^{(4)}(0)$ is shown in Fig. 6, together with the theoretical curves for different average photon numbers $\langle \hat{n} \rangle$. The measured data is normalized to $\gamma^{(4)}(\tau \gg \tau_c)$ with τ_c the coherence time of the quasithermal light. A quasithermal state generated in the laboratory, by letting a laser transmit through
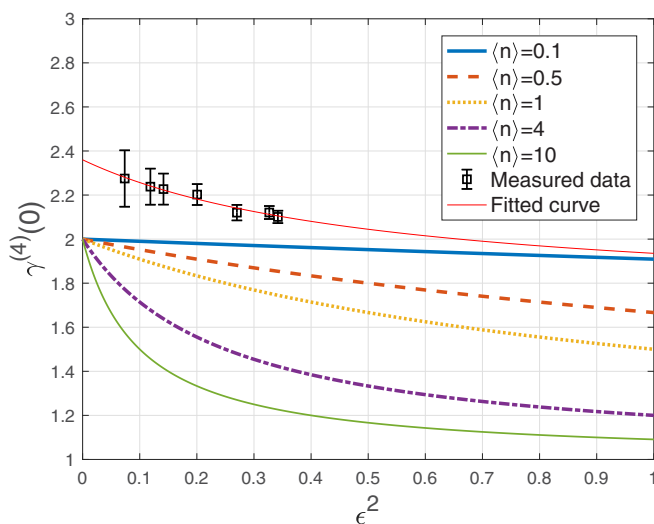

FIG. 6. Thermal state: calculated normalized coincidences $\gamma^{(4)}(0)$ for thermal states with varying $\langle \hat{n} \rangle$. Measured data from a quasithermal state (black squares, bars represent statistical errors), and the best fit to a rational (red, details in text). Here we assume $\eta_1^2 \mu_1^2 = \eta_2^2 \mu_2^2$ bunched into the expression ϵ^2 for simplicity.
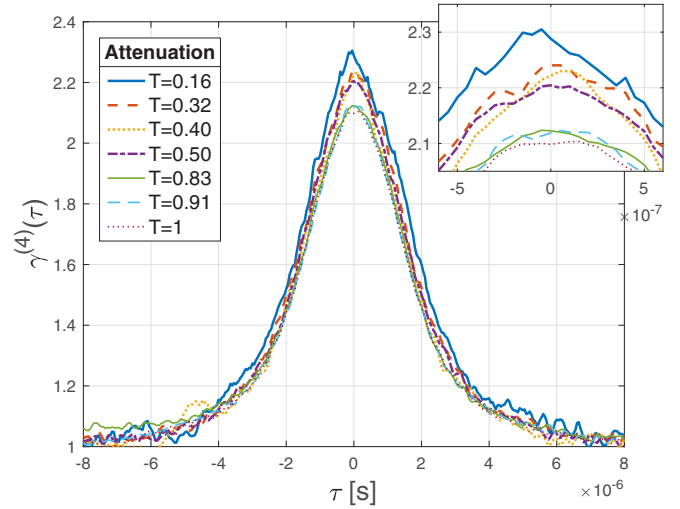

FIG. 7. Quasithermal state: Measured $\gamma^{(4)}(\tau)$, for several attenuation strengths (T=transmission through filter). Inset: enlargement around $\tau = 0$.

or scatter from a diffuser, does not in general have the exact exponential distribution over number states as described in the previous section, and thus the fourth-order correlation function can differ from 2. In our case the generated state is "superthermal," i.e., $g^{(4)}(0) > 2$, as can be seen in Fig. 6. The extra bunching cannot be explained by excess noise in the HeNe laser, this has been checked. Because of the super-thermal statistics we cannot map the measured data directly to the theoretical curves. However, we can see the expected trend: $\gamma^{(4)}(0)$ increases with increased attenuation. A curve with a best fit to the data can be made if we assume a similar ϵ^2 dependency as for a thermal state, and thus apply a rational of the form $y = (p_1 x + p_2)/(x + q_1)$ as indicated by the ratio of Eq. (22) to (23). This provides a "correction term" to the theoretical expression of $\gamma^{(4)}$ for a thermal state, accounting for the non-Gaussianity of the generated, super-thermal state. The best fit is plotted in Fig. 6 (red, solid curve), and indicates a correct value for $g^{(4)}(0) \simeq 2.36$. Thus, applying the method of varying the attenuation of the source while keeping all other factors constant allows us to determine a more accurate value for $g^{(4)}(0)$ compared to a single measurement.

In Fig. 7, the correlation function is plotted versus the difference τ in arrival time of photons, for different attenuation strengths. As for the coherent state, the x axis ϵ^2 in Fig. 6 is scaled to include estimated losses in the fiber, at the detector, and from the added attenuation. $\langle \hat{n} \rangle$, as it is presented in the plot, thus represents the average photon number of the mode after coupling the light into the fiber (before attenuation). The average photon number for the mode generated at the diffuser can be estimated to be in the range 100–1000 photons per mode (based on diffuser, beam, and fiber properties), but is spatially filtered to ensure coupling of one single mode into the fiber.

VIII. SYSTEMATIC VS STATISTICAL ERRORS

In the above measurements the measurement time was fixed, leading to increased statistical errors for higher attenuation.

That is, the proposed method decreases the systematic error $\gamma^{(4)}(\epsilon^2) - g^{(4)}(0)$ at the cost of an increased statistical error. In some measurements, statistical errors pose a significant problem, but in many cases it is manageable by increasing the measurement time, and preferred in relation to systematic errors.

For a fixed measurement time or number of measurements M of a pulsed source, there is a tradeoff between systematic and statistical errors. The latter can be derived from Eqs. (13) and (14) and are $(\sqrt{M}\epsilon^2 n)^{-1}$ for a number state $|n\rangle$ and $2(\sqrt{M}\epsilon^2 \langle \hat{n} \rangle)^{-1}$ for a coherent state or a thermal state, under the assumption of equal losses in both arms, and where we are in agreement with Figs. 2–4 and 6 we have collected all losses into the factor ϵ^2. These error estimates should be compared to the systematic errors that are $([1 - 1/n]\epsilon^2)/2$, 0, and $-\epsilon^2 \langle \hat{n} \rangle$, for the respective states. Thus, it takes, e.g., $M \approx 4/(\epsilon^8 \langle \hat{n} \rangle^4)$ measurements to make the two error terms of a pulsed, thermal source equal.

IX. CONCLUSION

The fourth-order correlation function is an important tool for characterizing nonclassical and classical light sources. It has long been a challenge to measure the characteristics of especially quantum light-source emitting states with more than one or two photons. The performance of current photon number resolving detectors is not satisfying, and setups for spacial or time multiplexing quickly become unpractical. As the efficiencies of detectors and setups improve, it is also important to keep in mind that what is normally measured in the laboratory is not the $g^{(4)}$ function, but an approximation only true under certain experimental conditions, notably low quantum efficiencies. Here, we have attempted to clarify how a measurement of the fourth-order correlation function is affected by experimental conditions, and specifically linear loss. We have shown that introducing and varying an excess attenuation can be a powerful and simple strategy to acquire information about the fourth-order correlation function $g^{(4)}(\tau)$ of any state. Attenuation can decrease a troubling systematic error in correlation measurements, at the expense of an increased statistical error, which may be easier to handle. Furthermore, we have experimentally demonstrated the feasibility of the method for a coherent state and a quasithermal state. The method is easy to implement and can simplify characterization of, for example, multiphoton Fock states as they become experimentally available. Future work includes experimentally verifying the method for a larger set of states.

ACKNOWLEDGMENTS

[1] R. Hanbury Brown and R. Q. Twiss, Nature **178**, 1046 (1956).

[2] R. J. Glauber, Phys. Rev. **130**, 2529 (1963).

[3] D. C. Burnham and D. L. Weinberg, Phys. Rev. Lett. **25**, 84 (1970).

[4] H. J. Kimble, M. Dagenais, and L. Mandel, Phys. Rev. Lett. **39**, 691 (1977).

[5] C. K. Hong, Z. Y. Ou, and L. Mandel, Phys. Rev. Lett. **59**, 2044 (1987).

[6] F. Diedrich and H. Walther, Phys. Rev. Lett. **58**, 203 (1987).

[7] P. Michler, A. Kiraz, C. Becher, W. V. Schoenfeld, P. M. Petroff, L. Zhang, E. Hu, and A. İmamoğlu, Science **290**, 2282 (2000).

[8] C. Santori, D. Fattal, J. Vučković, G. S. Solomon, and Y. Yamamoto, Nature **419**, 594 (2002).

[9] B. Darquié, M. P. A. Jones, J. Dingjan, J. Beugnon, S. Bergamini, Y. Sortais, G. Messin, A. Browaeys, and P. Grangier, Science **309**, 454 (2005).

[10] L. Mandel, Proc. Phys. Soc. **72**, 1037 (1958).

[11] L. Mandel and E. Wolf, Rev. Mod. Phys. **37**, 231 (1965).

[12] F. Arecchi, E. Gatti, and A. Sona, Phys. Lett. **20**, 27 (1966).

[13] F. Davidson and L. Mandel, J. Appl. Phys. **39**, 62 (1968).

[14] L. Mandel and E. Wolf, *Optical Coherence and Quantum Optics* (Cambridge University, Cambridge, England, 1995).

[15] I. N. Agafonov, M. V. Chekhova, T. S. Iskhakov, and A. N. Penin, Phys. Rev. A **77**, 053801 (2008).

[16] T. S. Iskhakov, A. M. Pérez, K. Y. Spasibko, M. V. Chekhova, and G. Leuchs, Opt. Lett. **37**, 1919 (2012).

[17] F. Boitier, A. Godard, E. Rosencher, and C. Fabre, Nat. Phys. **5**, 267 (2009).

[18] Y. Yamamoto and H. A. Haus, Rev. Mod. Phys. **58**, 1001 (1986).

[19] C. M. Caves and P. D. Drummond, Rev. Mod. Phys. **66**, 481 (1994).

[20] A. Ourjoumtsev, H. Jeong, R. Tualle-Brouri, and P. Grangier, Nature **448**, 784 (2007).

[21] M. J. Holland and K. Burnett, Phys. Rev. Lett. **71**, 1355 (1993).

[22] J.-W. Pan, D. Bouwmeester, M. Daniell, H. Weinfurter, and A. Zeilinger, Nature **403**, 515 (2000).

[23] F. W. Sun, B. H. Liu, Y. X. Gong, Y. F. Huang, Z. Y. Ou, and G. C. Guo, Europhys. Lett. **82**, 24001 (2008).

[24] F. Mattioli, Z. Zhou, A. Gaggero, R. Gaudio, S. Jahanmirinejad, D. Sahin, F. Marsili, R. Leoni, and A. Fiore, Supercond. Sci. Technol. **28**, 104001 (2015).

[25] R. Heilmann, J. Sperling, A. Perez-Leija, M. Gräfe, M. Heinrich, S. Nolte, W. Vogel, and A. Szameit, Sci. Rep. **6**, 19489 (2016).

[26] J.-W. Pan, M. Daniell, S. Gasparoni, G. Weihs, and A. Zeilinger, Phys. Rev. Lett. **86**, 4435 (2001).

[27] Z. Zhao, Y.-A. Chen, A.-N. Zhang, T. Yang, H. J. Briegel, and J.-W. Pan, Nature **430**, 54 (2004).

[28] X.-C. Yao, T.-X. Wang, P. Xu, H. Lu, G.-S. Pan, X.-H. Bao, C.-Z. Peng, C.-Y. Lu, Y.-A. Chen, and J.-W. Pan, Nat. Photon. **6**, 225 (2012).

[29] X.-L. Wang, L.-K. Chen, W. Li, H.-L. Huang, C. Liu, C. Chen, Y.-H. Luo, Z.-E. Su, D. Wu, Z.-D. Li, H. Lu, Y. Hu, X. Jiang, C.-Z. Peng, L. Li, N.-L. Liu, Y.-A. Chen, C.-Y. Lu, and J.-W. Pan, Phys. Rev. Lett. **117**, 210502 (2016).

[30] I. Straka, L. Lachman, J. Hloušek, M. Miková, M. Mičuda, M. Ježek, and R. Filip, npj Quantum Inform. **4**, 4 (2018).

[31] T. S. Iskhakov, O. A. Ivanova, and M. V. Chekhova, in *Proceedings of the SPIE 5833*, Quantum Informatics 2004, edited by Y. I. Ozhigov (SPIE, New York, 2005).

[32] M. Avenhaus, K. Laiho, M. V. Chekhova, and C. Silberhorn, Phys. Rev. Lett. **104**, 063602 (2010).

[33] M. Cooper, L. J. Wright, C. Söller, and B. J. Smith, Opt. Express **21**, 5309 (2013).

[34] G. Zambra, A. Andreoni, M. Bondani, M. Gramegna, M. Genovese, G. Brida, A. Rossi, and M. G. A. Paris, Phys. Rev. Lett. **95**, 063602 (2005).

[35] I. Straka, A. Predojević, T. Huber, L. Lachman, L. Butschek, M. Miková, M. Mičuda, G. S. Solomon, G. Weihs, M. Ježek, and R. Filip, Phys. Rev. Lett. **113**, 223603 (2014).